

# The colors of satellite galaxies in the Illustris Simulation

Laura V. Sales<sup>1\*</sup>, Mark Vogelsberger<sup>2</sup>, Shy Genel<sup>1</sup>, Paul Torrey<sup>1,2</sup>, Dylan Nelson<sup>1</sup>, Vicente Rodriguez-Gomez<sup>1</sup>, Wenting Wang<sup>3</sup>, Annalisa Pillepich<sup>1</sup>, Debora Sijacki<sup>4</sup>, Volker Springel<sup>5,6</sup> and Lars Hernquist<sup>1</sup>

<sup>1</sup>Harvard-Smithsonian Center for Astrophysics, 60 Garden Street, Cambridge, MA, 02138, USA

<sup>2</sup>Department of Physics, Kavli Institute for Astrophysics and Space Research, Massachusetts Institute of Technology, Cambridge, MA 02139, USA

<sup>3</sup>Institute for Computational Cosmology, University of Durham, South Road, Durham DH1 3LE

<sup>4</sup>Institute of Astronomy and Kavli Institute for Cosmology, University of Cambridge, Madingley Road, Cambridge CB3 0HA, UK

<sup>5</sup>Heidelberg Institute for Theoretical Studies, Schloss-Wolfsbrunnengasse 35, D-69118 Heidelberg, Germany

<sup>6</sup>Zentrum fuer Astronomie der Universitaet Heidelberg, ARI, Muenchhofstr. 12-14, D-69120 Heidelberg, Germany

29 October 2014

## ABSTRACT

Observationally, the fraction of blue satellite galaxies decreases steeply with host halo mass, and their radial distribution around central galaxies is significantly shallower in massive ( $M_* \geq 10^{11} M_\odot$ ) than in Milky Way like systems. Theoretical models, based primarily on semi-analytical techniques, have had a long-standing problem with reproducing these trends, instead predicting too few blue satellites in general but also estimating a radial distribution that is too shallow, regardless of primary mass. In this Letter, we use the Illustris cosmological simulation to study the properties of satellite galaxies around isolated primaries. For the first time, we find good agreement between theory and observations. We identify the main source of this success relative to earlier work to be a consequence of the large gas contents of satellites at infall, a factor  $\sim 5$ -10 times larger than in semi-analytical models. Because of their relatively large gas reservoirs, satellites can continue to form stars long after infall, with a typical timescale for star-formation to be quenched  $\sim 2$  Gyr in groups but more than  $\sim 5$  Gyr for satellites around Milky Way like primaries. The gas contents we infer are consistent with  $z = 0$  observations of HI gas in galaxies, although we find large discrepancies among reported values in the literature. A testable prediction of our model is that the gas-to-stellar mass ratio of satellite progenitors should vary only weakly with cosmic time.

**Key words:** galaxies: structure, galaxies:haloes, galaxies: evolution

## 1 INTRODUCTION

The observed properties of satellite galaxies can provide insight on a number of processes related to their environments, and provide clues about the intrinsic properties of these objects when they were first accreted by their hosts. Galaxies that orbit within larger gravitational potentials are subject to a variety of physical effects that can significantly decrease their star formation activity, including tidal and ram-pressure stripping and the suppression of a supply of fresh gas. Reddening, mass loss, and morphological transformations are among the most likely outcomes in response to such environmental effects. Moreover, the strength of these processes will typically decrease at large distance to the host halo center.

Observationally, it is found that satellite galaxies have a projected number density distribution close to a power law (e.g., Sales & Lambas 2005; van den Bosch et al. 2005; Tal et al. 2012; Nierenberg et al. 2012; Jiang et al. 2012), that is similar to the steep distribution of dark matter expected in their hosts. But, when split by color, it is expected that blue/star-forming objects should be under-represented in the inner regions, leading to a shallower radial distribution of blue satellites compared to the red population. Observations suggest that this is indeed the case for satellites orbiting groups and clusters with relatively massive primaries. However, for systems with a central galaxy of intermediate to low stellar mass, most of the satellites with stellar masses above  $\sim 10^8 M_\odot$  are blue, including those in the inner regions (Prescott et al. 2011; Wetzel et al. 2012; Guo et al. 2013; Wang et al. 2014).

Significant theoretical effort has been devoted to reproducing these trends with satellite colors. A fair comparison with observa-

\* E-mail: lsales@cfa.harvard.edu

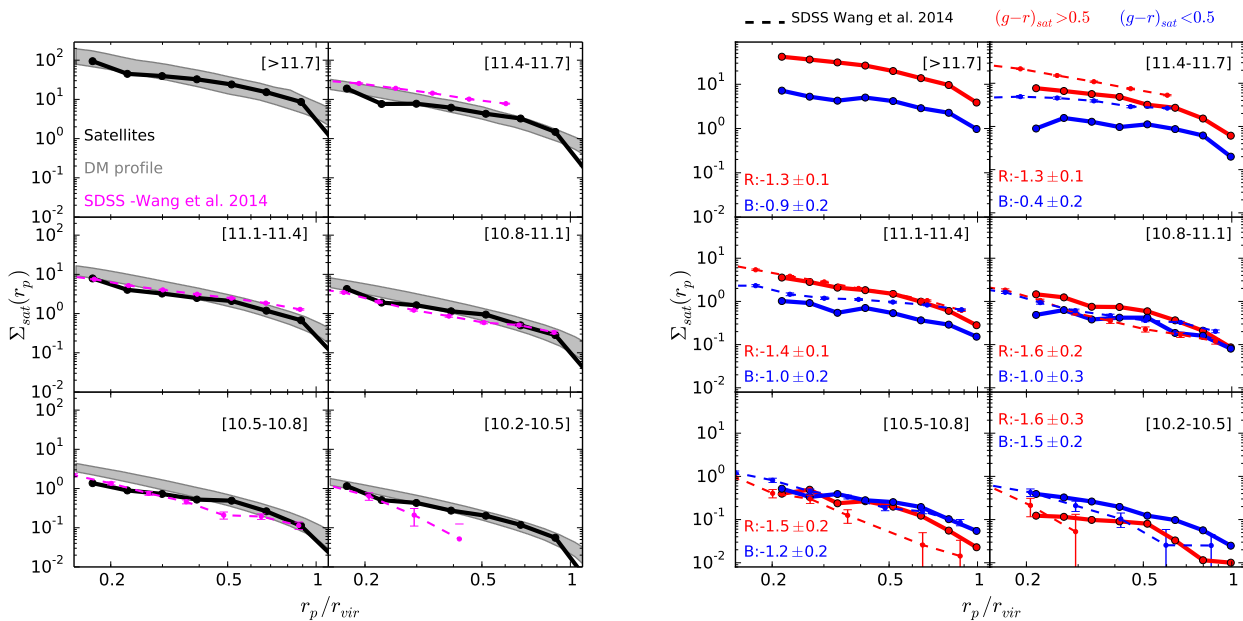


**Figure 1.** *Left:* Projected number density profile of satellites,  $\Sigma_{\text{sat}}$ , in Illustris. Panels correspond to different primary galaxy stellar masses, as indicated (in log-scale). Satellites approximately follow the distribution of dark matter particles in their host halos, as shown by the grey shaded area corresponding to the 25%-75% percentiles of the sample (arbitrarily re-normalised such that satellites and DM profiles intersect at  $r_p/r_{\text{vir}} = 0.5$ ). Dashed magenta lines show results from the SDSS analysis presented in Wang et al. (2014). *Right:* Same as left panel, but satellites are divided into red and blue populations. Fits to the profiles’ slopes are quoted in each panel. Our simulations (solid) successfully reproduce two key aspects of the SDSS results (dashed): *i*) a dominant red/blue population for high/low mass primaries and *ii*) a steep profile of the blue satellites orbiting low mass primaries (bottom row).

tions requires a large number of systems to be analysed, motivating the use of semi-analytical catalogs and *ad-hoc* tagging techniques preferable over hydrodynamic simulations. However, these models consistently appear to overestimate the fraction of red satellites and fail to reproduce the steep slopes of the blue population around low mass primaries (Weinmann et al. 2006; Kimm et al. 2009; Guo et al. 2013; Wang et al. 2014). This has traditionally been attributed to an overestimate of environmental effects, possibly related to an improper handling of cold/hot gas evolution in satellites leading to overly rapid quenching (Font et al. 2008; Kang & van den Bosch 2008; Weinmann et al. 2010; Kimm et al. 2011). However, by suppressing all environmental effects Wang et al. (2014) recently showed that while this would increase the fraction of blue satellites, their radial distribution would still be significantly shallower than observed. The main difficulty seems to be in fueling star formation for several Gyrs after a satellite has been accreted by its primary host.

In what follows, we examine the distribution of satellites by color using the recently completed hydrodynamical simulation “Illustris”. Our results offer a new perspective on the issues at hand by self-consistently following the details of internally- and externally-driven evolution of satellites, explicitly accounting for both their dark matter and baryonic components.

## 2 NUMERICAL SIMULATIONS

Satellite and primary galaxies are selected from the “Illustris” hydrodynamical simulation<sup>1</sup> (Vogelsberger et al. 2014a,b; Genel et

al. 2014). This simulation is based on a large cosmic volume (106.5 Mpc on a side) with global properties consistent with a WMAP-9 cosmology (Hinshaw et al. 2013) and evolved using the moving-mesh code AREPO (Springel 2010). Dark matter, gas and stars are followed from redshift  $z = 127$  to  $z = 0$ . The simulation includes a treatment of the astrophysical processes thought to be most important for the formation and evolution of galaxies, such as gravity, gas cooling/heating, star formation, mass return and metal enrichment from stellar evolution, and feedback from stars and supermassive black holes. The model reproduces a number of key observable properties of the galaxy population at the present-day and at higher redshifts, including stellar mass functions, scaling relations, color distributions, and the morphological diversity of galaxies.

Individual objects in the simulation are identified using the SUBFIND algorithm (Springel et al. 2001; Dolag et al. 2009) and are divided into “central” and “satellite” galaxies according to their rank within their friends-of-friends (FoF) group, so that the “central” object corresponds (in their majority) to the most massive subhalo of the group. In what follows, we consider all *central* galaxies with stellar mass  $M_* > 10^{10} M_\odot$  as isolated primaries and study the distribution and color of their surrounding *satellites* that belong to their FoF groups and that are more massive than  $M_* > 10^8 M_\odot$ . At the resolution of the simulation (mass per particle  $m_p = 6.3 \times 10^6 M_\odot$  and  $1.3 \times 10^6 M_\odot$  for dark matter and baryons, gravitational softening  $\epsilon \sim 500$  at  $z = 0$ ), all such “satellites” are resolved with  $\sim 100$  or more stellar particles. Stellar/gas mass and  $(g-r)$  colors of simulated galaxies are measured within twice the stellar half mass radius. Virial quantities correspond to the radius where the spherically-averaged inner density is 200 times the critical density of the Universe.

<sup>1</sup> <http://www.illustris-project.org>

Our simulations track the evolution of satellite galaxies self-consistently, combining internal processes such as star formation and feedback with external effects due to the environment, such as tidal stripping, dynamical friction, ram-pressure, gas compression by shocks, etc. The AREPO code is well suited to handle the fluid and gravitational instabilities expected to arise in such complex configurations, with the creation of hot bubbles due to stellar/AGN winds, gaseous tails due to ram pressure, stellar streams and shells. We have used a lower resolution box to confirm that the results do not depend strongly on resolution. Our sample comprises 9529 satellites around 3306 primary galaxies at  $z = 0$ .

### 3 RESULTS

The left panel of Fig. 1 shows the projected radial distribution of satellites around primaries in different stellar mass bins, as indicated in each panel (in log-scale). We consider all satellites that are within the 3D virial radius of their hosts (taking all satellites in the FoF group changes only slightly the outer regions). The projected profiles,  $\Sigma_{\text{sat}}$  (black solid lines), correspond to the average number of satellites found per primary at a given projected separation  $r_p$  (direction of projection chosen randomly) and normalised to the virial radius of the host halo  $r_{\text{vir}}$ . An interesting outcome is seen by comparing this with the shaded grey area which shows the 25%-75% distribution for the dark matter profiles in these halos (normalised arbitrarily so that they intersect at  $r_p/r_{\text{vir}} = 0.5$ ). We find that satellite galaxies roughly follow the underlying distribution of dark matter in the distance range  $0.2 \leq r_p/r_{\text{vir}} < 1$ , with a trend to flatten towards the inner regions. Previous works have shown no consensus on this issue, although most of the discrepancies might be explained by different selection criteria and distance range considered (see Section 1, Wang et al. (2014)).

The left panel of Fig. 1 also shows (dashed magenta lines) observational results based on photometric and spectroscopic SDSS data from Wang et al. (2014). In this work, primaries are identified following isolation criteria for their projected distance and redshift distributions, while satellite profiles result from the photometric SDSS sample after properly accounting for background/foreground objects through a subtraction method. Stellar mass cuts in primaries and satellites are similar to our analysis. The good agreement between the slopes and normalisations of the black solid and dashed magenta lines is encouraging, especially taking into account the different selection criteria used in the two samples. (For the least massive bins, the background subtraction method and the isolation criteria can have a significant impact on the profile slopes obtained; see Appendix in Wang et al.)

We explore satellite profiles split by color in the right panel of Fig. 1. Here, we adopt a uniform color cut  $(g-r) = 0.5$  independent of satellite mass, but we have explicitly checked that this choice does not qualitatively bias our results. For the most massive primaries ( $\log(M_*/M_\odot) > 11$ ) red satellites dominate the overall population and tend to be distributed more steeply than the blue ones, especially for the four most massive primary bins. However, in lower mass systems, satellites are predominantly blue and exhibit a steeper radial profile than in more massive systems. We quote in each panel the slope found for each population and its uncertainty based on 100 bootstrap resamplings of the data. These trends agree well with observations, including the SDSS results of Wang et al. (2014) – shown here by the red/blue dashed lines (see also Guo

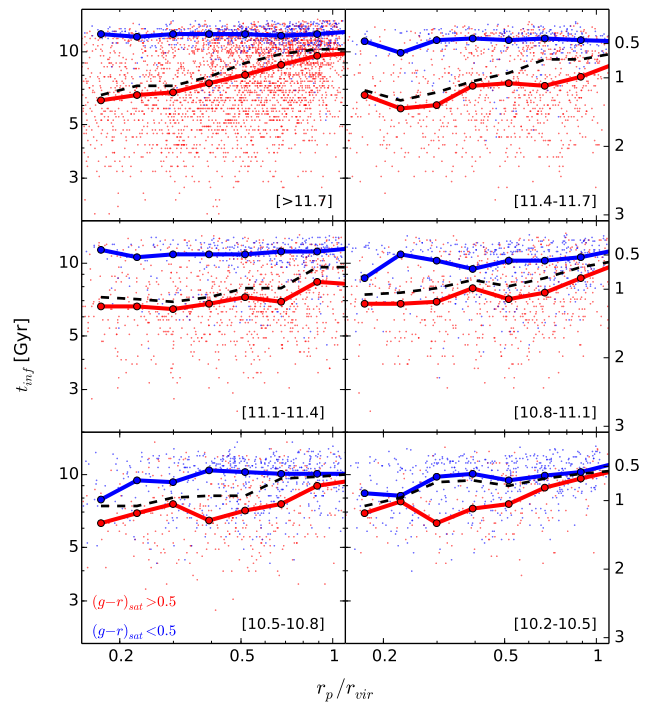


**Figure 2.** Infall times  $t_{\text{inf}}$  for satellites as a function of present-day projected distance (right y-axes display corresponding redshifts). Points indicate individual satellites and red/blue corresponds to their  $(g-r)$  colors at  $z = 0$ . The median trend considering all satellites is shown by the black dashed lines and is roughly independent of the primary stellar mass (different panels). However, when split by color (solid curves), satellites that remain blue today can have significantly earlier infall times in low mass primaries (bottom two panels) than in more massive hosts.

et al. 2013). Reproducing these behaviours and the abundance of blue satellites around low mass primaries has been a challenge in theoretical models of galaxy formation based on semi-analytical methods, but they seem to arise naturally in our simulations.

Variations in satellite infall times for a wide range of primary masses could explain their different color distributions. However, we find that  $t_{\text{inf}}$  is roughly independent of primary mass, as shown by the median relations (black dashed curves) in Fig. 2. We define  $t_{\text{inf}}$  as the last time a satellite was a central galaxy of its own FoF group, and explicitly checked that using a different definition (e.g., the time when the satellite joins the FoF group to which it belongs at  $z = 0$ ) yields similar results. When we split satellites by their own colors we find large differences. In the most massive systems, regardless of the projected distance of the satellite, blue objects have typically fallen in only recently, fewer than  $\sim 2$  Gyrs ago. Instead, for primaries comparable to the Milky Way, the median infall time of blue satellites in the inner regions is  $\sim 5$  Gyrs ago, with individual cases scattering down to  $> 7$  Gyrs.

Interestingly, red satellites cease forming stars on very different timescales according to their orbits: they show slow gas consumption in wide orbits to rapid single pericenter episodes for very radial ones. In general, surviving satellites maintain a similar stellar mass to that at infall, although a few percent (2%-10%, depending on primary mass) more than double their stellar content during their lives as satellites (see also Pillepich et al. 2014). Apprecia-

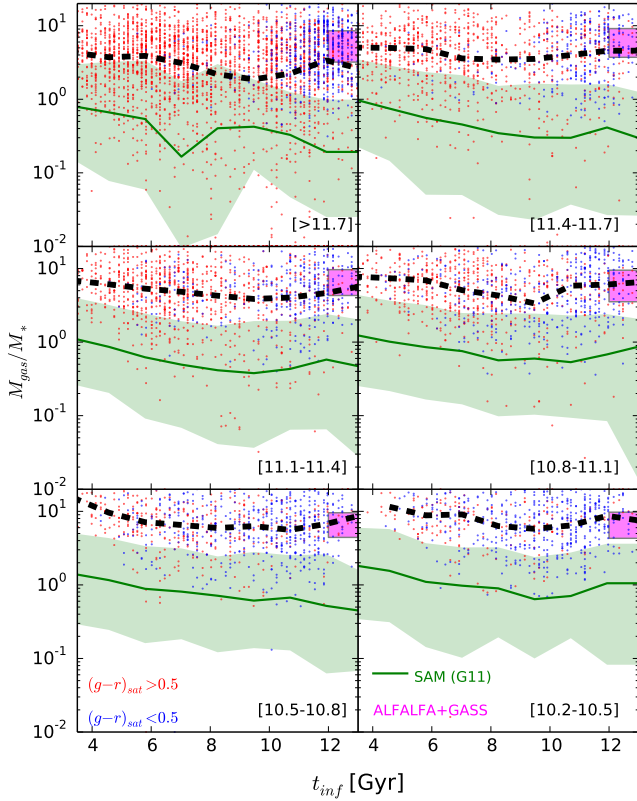


**Figure 3.** Satellite gas-to-stellar mass ratios at infall,  $M_{\text{gas}}/M_*$ , as a function of infall time. As earlier, the panels correspond to different primary stellar masses, red/blue denotes  $(g-r)$  colors of satellites at  $z = 0$  and the median trend is shown by the black dashed curves. (The vertical stripes in the points distribution reflect the finite number of output times.) In Illustris, satellites infall with a large gas content ( $M_{\text{gas}}/M_* \sim 2-8$ ) that allows them to form stars for several Gyrs. The gas contents in our model are, at present epoch, in good agreement with observational estimates from the ALFALFA and GASS surveys (magenta rectangles; see text for more details). The green shaded region indicates gas-to-stellar mass ratios adopted in semi-analytical models (in this case taken from Guo et al. 2011), which are substantially lower than in our simulations. This appears to be a key factor to explaining the overproduction of red satellites in SAMs.

ble stellar stripping occurs only for red satellites, but the impact is small; fewer than 3% have lost at least half their initial stellar mass. These results are in reasonably good agreement with the standard treatment of star formation in satellite galaxies employed in semi-analytical models.

We find that a key factor in achieving a prolonged star formation for satellites in Fig. 2 (and therefore, producing the good match between observed satellite colors/distribution) is the large gas contents of satellites at infall. Fig. 3 shows, in bins of primary stellar mass, the infall gas-to-stellar mass ratios  $M_{\text{gas}}/M_*$  of satellites as a function of their infall times. We consider all gas particles within twice the stellar half-mass radius and we have checked that it is dominated (in more than 90%) by the cold ( $T < 2 \times 10^4$  K) plus star-forming components. The median in our simulations suggests that, at infall, satellites have  $\sim 2-5$  times more gas than stars. We also find a weak trend of  $M_{\text{gas}}/M_*$  with the primary stellar mass (different panels), that is a consequence of the most massive systems having more massive satellites, which are, on average, less gas-rich than the lower mass dwarfs that dominate the satel-

ite population of intermediate and low mass primaries (see Fig. 3 in Vogelsberger et al. (2014a) for the mass-dependent nature of gas contents in our simulations and observations).

To relate our finding with previous results in the literature, we compare our simulated gas contents with those from the publicly available semi-analytical model of Guo et al. (2011), which has itself (or its predecessors) been extensively used in the study of satellite galaxy properties. We select primaries and satellites from the Millennium-II volume (Boylan-Kolchin et al. 2009) with the exact same selection criteria as employed in analysing our simulations. The median (green solid line) and 10%-90% percentiles (shaded area) of the distribution of cold gas-to-stellar mass ratios in the SAM are shown in Fig. 3. The difference with the simulated data is striking, in the sense that the galaxies are approximately a factor 10 times less gas-rich in the semi-analytical catalog than in Illustris. We have checked that this is independent of satellite stellar mass and is also present for *central* galaxies in the model. On this basis, we argue that the relatively low gas content of satellites at infall in the semi-analytical models is largely responsible for their failure to reproduce the color and distribution of satellite galaxies.

Unbiased observational estimates of gas contents are challenging, specially for low mass objects. Gas fractions reported in the literature show large variations depending on the observational strategy. Optically selected samples find systematically lower gas fractions than HI-selected samples like ALFALFA (see Papastergis et al. 2012). Ideally, the best constraints should come from mass-complete, optically selected samples like GASS (Catinella et al. 2010). However, presently these surveys are restricted to only massive galaxies ( $M_* > 10^{10} M_\odot$ ). Because low-mass central galaxies are mostly star-forming, we assume that satellites before infall follow ALFALFA reported gas fractions from Huang et al. (2012) if  $M_* < 10^{10} M_\odot$  but that of GASS if they are more massive. The magenta rectangles in Fig. 3 indicate the gas-to-stellar mass ratios obtained by assigning to each simulated satellite with a recent infall time ( $t_{\text{inf}} > 12$  Gyr) the gas content according to this ALFALFA+GASS combination, a 0.3 dex dispersion around the mean, and assuming a mass-independent molecular fraction of 0.3 (Saintonge et al. 2011). The simulated values are in good agreement with what would be expected from such observations at  $z = 0$ .

Lastly, since the parameters in the model used in Illustris were not calibrated to reproduce gas quantities, the weak dependence of the (total) gas-to-stellar ratio with infall redshift is actually a prediction of our model. Interestingly, an independent analysis of the stellar mass - metallicity relations at several redshifts (Zahid et al. 2014) also seems to indicate such a weak evolution.

## 4 CONCLUSION

We use the Illustris cosmological simulation to study the distribution of satellite galaxies around isolated primaries. The large volume of our simulated box allows us to statistically characterise  $\sim 9500$  satellite galaxies with  $M_* > 10^8 M_\odot$  orbiting primaries with masses comparable to the Milky Way and above. This is the first time such a study has been performed using a hydrodynamical simulation.

We find good agreement between our results and observations from the SDSS wide field survey. In our simulations, *i*) satellites roughly trace the distribution of dark matter in their hosts, and *ii*) in high-mass systems, red satellites dominate and are distributed more steeply than the blue population, whereas for lower mass primaries, satellites are mostly blue and they also follow a steep number den-

sity profile. This good agreement with the observations contrasts with earlier theoretical modeling, mostly based on semi-analytical techniques, which were unable to reproduce the satellite color - primary mass dependent behaviour seen in the observations. Based on the semi-analytical model output of Guo et al. (2011), we suggest that gas contents that are too low for satellites at infall (and not the modelling of environmental effects) is the most likely cause of the challenges faced by such models in reproducing observations.

Our simulations provide a tool for understanding the timescales for the quenching of star formation in different environments. At infall, simulated satellites carry significant amounts of gas, with quartiles  $M_{\text{gas}}/M_* = 2-8$ , that can fuel star formation for long periods of time. Moreover, we find a very weak evolution of gas-to-stellar mass ratios with redshift, a testable prediction of the model that can be explored once observational estimates of total gas mass become available for galaxies at higher redshifts.

## ACKNOWLEDGEMENTS

We are grateful to the anonymous referee for a constructive and positive report that helped improve the previous version of this letter. LVS wishes to thank Simon White and Guinnevere Kauffmann for stimulating discussions and Manolis Papastergis for facilitating ALFALFA tables. Simulations were run on the Harvard Odyssey and CfA/ITC clusters, the Ranger and Stampede supercomputers at the Texas Advanced Computing Center as part of XSEDE, the Kraken supercomputer at Oak Ridge National Laboratory as part of XSEDE, the CURIE supercomputer at CEA/France as part of PRACE project RA0844, and the SuperMUC computer at the Leibniz Computing Centre, Germany, as part of project pr85je. L.H. acknowledges support from NASA grant NNX12AC67G and NSF grant AST-1312095. V.S. acknowledges support from the European Research Council through ERC-StG grant EXAGAL-308037.

## REFERENCES

- Boylan-Kolchin M., Springel V., White S. D. M., Jenkins A., Lemson G., 2009, *MNRAS*, 398, 1150
- Catinella B., Schiminovich D., Kauffmann G., Fabello S., Wang J., et al. 2010, *MNRAS*, 403, 683
- Dolag K., Borgani S., Murante G., Springel V., 2009, *MNRAS*, 399, 497
- Font A. S., Bower R. G., McCarthy I. G., Benson A. J., Frenk C. S., Helly J. C., Lacey C. G., Baugh C. M., Cole S., 2008, *MNRAS*, 389, 1619
- Genel S., Vogelsberger M., Springel V., Sijacki D., Nelson D., Snyder G., Rodriguez-Gomez V., Torrey P., Hernquist L., 2014, *MNRAS*, 445, 175
- Guo Q., Cole S., Eke V., Frenk C., Helly J., 2013, *MNRAS*, 434, 1838
- Guo Q., White S., Boylan-Kolchin M., De Lucia G., Kauffmann G., Lemson G., Li C., Springel V., Weinmann S., 2011, *MNRAS*, 413, 101
- Hinshaw G., Larson D., Komatsu E., Spergel D. N., et al. 2013, *ApJS*, 208, 19
- Huang S., Haynes M. P., Giovanelli R., Brinchmann J., 2012, *ApJ*, 756, 113
- Jiang C. Y., Jing Y. P., Li C., 2012, *ApJ*, 760, 16
- Kang X., van den Bosch F. C., 2008, *ApJL*, 676, L101
- Kimm T., Somerville R. S., Yi S. K., van den Bosch F. C., Salim S., Fontanot F., Monaco P., Mo H., Pasquali A., Rich R. M., Yang X., 2009, *MNRAS*, 394, 1131
- Kimm T., Yi S. K., Khochfar S., 2011, *ApJ*, 729, 11
- Nierenberg A. M., Auger M. W., Treu T., Marshall P. J., Fassnacht C. D., Busha M. T., 2012, *ApJ*, 752, 99
- Papastergis E., Cattaneo A., Huang S., Giovanelli R., Haynes M. P., 2012, *ApJ*, 759, 138
- Pillepich A., Madau P., Mayer L., 2014, *ArXiv e-prints* 1407.7855
- Prescott M., et al., 2011, *MNRAS*, 417, 1374
- Saintonge A., Kauffmann G., Kramer C., Tacconi L. J., Buchbender C., et al. 2011, *MNRAS*, 415, 32
- Sales L., Lambas D. G., 2005, *MNRAS*, 356, 1045
- Springel V., 2010, *MNRAS*, 401, 791
- Springel V., White S. D. M., Tormen G., Kauffmann G., 2001, *MNRAS*, 328, 726
- Tal T., Wake D. A., van Dokkum P. G., 2012, *ApJL*, 751, L5
- Torrey P., Vogelsberger M., Genel S., Sijacki D., Springel V., Hernquist L., 2014, *MNRAS*, 438, 1985
- van den Bosch F. C., Yang X., Mo H. J., Norberg P., 2005, *MNRAS*, 356, 1233
- Vogelsberger M., Genel S., Springel V., Torrey P., Sijacki D., Xu D., Snyder G., Bird S., Nelson D., Hernquist L., 2014, *Nature*, 509, 177
- Vogelsberger M., Genel S., Springel V., Torrey P., Sijacki D., Xu D., Snyder G., Nelson D., Hernquist L., 2014, *MNRAS*, 444, 1518
- Wang W., Sales L. V., Henriques B. M. B., White S. D. M., 2014, *MNRAS*, 442, 1363
- Weinmann S. M., Kauffmann G., von der Linden A., De Lucia G., 2010, *MNRAS*, 406, 2249
- Weinmann S. M., van den Bosch F. C., Yang X., Mo H. J., Croton D. J., Moore B., 2006, *MNRAS*, 372, 1161
- Wetzel A. R., Tinker J. L., Conroy C., 2012, *MNRAS*, 424, 232
- Zahid H. J., Dima G. I., Kudritzki R.-P., Kewley L. J., Geller M. J., Hwang H. S., Silverman J. D., Kashino D., 2014, *ApJ*, 791, 130